Electronic Supporting Information

A Graphene Dispersed CdS-MoS_2 Nanocrystal Ensemble for Cooperative Photocatalytic Hydrogen Production from Water

Tiantian Serena Jia,[a] Amy Kolpin,[a] Chensheng Ma,[b] Ruth Chau-Ting Chan[c] Wai-Ming Kwok[c] and Shik Chi Edman Tsang [a,*]

[a.] *Department of Chemistry, University of Oxford, Oxford, OX1 3QR, United Kingdom*
[b.] *School of Chemistry and Chemical Engineering, Shenzhen University, Shenzhen, 518060, China*
[c.] *Department of Applied Biology and Chemical Technology, Hong Kong Polytechnic University, Hung Hom, Hong Kong.*

**Corresponding author, E-mail: edman.tsang@chem.ox.ac.uk*

Experimental Methods

1. Material Synthesis

1.1 Syntheisis of CdS nanoparticles

The spherical CdS nanoparticles were synthesized by the method described by Joo et. al.[1] In a typical procedure, 604 mg of cadmium chloride-1-hydrate (3 mmol) was well dissolved in 30 mL of oleylamine. Then, the mixture was transferred to a three-necked flask and was heated to 90 °C for 1 h. Thereafter, 48 mg of sulphur dissolved in 5 mL of oleylamine and was injected to the mixture. It was heated to 160 °C with vigorous stirring and N_2 protection for another 6 h. Finally, the resulting CdS nanoparticles were retrieved by adding acetone followed by centrifugation and washed at least three times with acetone and water to completely remove the solvent.

1.2 Synthesis of MoS_2

In a typical synthesis of MoS_2 nanoplates,[2] 1 mmol of $Na_2MoO_4 \cdot 2H_2O$ and 5 mmol of $CS(NH_2)_2$ were dissolved in 60 mL of distilled water. The homogeneous solution was then transferred into a 100 mL Teflon-lined autoclave and held at 210 °C for 24 h. After that, the black precipitate was collected by centrifugation, washed three times with distilled water and ethanol, and then dried in an oven at 80 °C for 12 h.

1.3 Synthesis of graphene oxide

Graphene was synthesized by an improved Hummers' method.[3, 4] For this method, a 9:1 mixture of concentrated H_2SO_4/H_3PO_4 (360:40 mL) was added to a mixture of graphite (3.0 g) and $KMnO_4$ (18.0 g). The mixture was heated to 50 °C and stirred for 12 h. Then the reaction was cooled to room temperature and poured onto ice (400 mL) with 30% H_2O_2 (3 mL). After stirring another 30 min, the mixture was centrifuged at 1000 rpm for 5 mins, and the precipitates were removed. This was repeated 4-5 times until no obvious precipitate was left after centrifuge. After that, the suspension was centrifuged at 8000 rpm for 15 mins and the supernatant was decanted away. The remaining solid material was then washed with 200 mL of water, 200 mL of 30% HCl, and 200 mL of ethanol successively. The material remaining after the wash process was vacuum-dried overnight (~12 h) at 80 °C.

1.4 Synthesis of nanocomposites

CdS-MoS_2 nanocomposites were prepared by mixing 100 mg CdS nanoparticles and different amounts of MoS_2. The mixture was then sonicated in 50 mL ethanol for 2 hours and stirred at room temperature for 24 hours.[5] CdS-Graphene-MoS_2 nanocomposites were prepared by mixing 100 mg CdS and different amounts of MoS_2 and graphene oxide in 50 mL ethanol. The composites were sonicated for 2 hours and stirred at room temperature for 24 hours. Detailed materials characterization and methodologies can be found in the S1 and Figure S9.

2. Materials Characterization

Transmission Electron Microscopy (TEM): A JEOL 2010 was used to record TEM images. The samples were sonicated 1 h in ethanol and dropped onto a lacey carbon coated copper grid, then dried in air at room temperature.

Powder X-Ray Diffraction (XRD): XRD analysis was performed using a PANalytical X'Pert Pro diffractormeter, operating in Bragg-Brentano focusing geometry and using Cu_{ka} radiation (λ = 1.5418 Å) from a generator operating at 40 kV and 40 mA. The sample powder was placed directly onto a glass slide and smoothed to form a thin uniform layer.

X-Ray Photoelectron Spectroscopy (XPS): XPS was performed in a VG Microtec ion pumped XPS system equipped with a nine channel CLAM4 electron energy analyser. 200 watt Mg X-ray excitation was used. The samples were analysed with reference to adventitious carbon 1s peak.

Electrochemical Measurements. Electrochemical measurements were performed using a 660 CHI electrochemical station. 5 mg of catalyst and 100 µl of 5 wt% Nafion solution were dispersed in 2 ml of 4:1 v/v water/ethanol by 1 h sonication to form a homogeneous suspension. Then about 5 µl of the catalyst ink was dropped onto a glassy carbon electrode 3 mm in diameter (loading ~ 0.71 mg/cm^2). A linear sweep from 0.2 to -0.6V and a scan rate of -2 mVs^{-1} was conducted in 0.5 M H_2SO_4 using a saturated calomel electrode as the reference electrode, a Pt wire as the counter electrode and the glassy carbon electrode as the working electrode.

Photocatalytic Test. Photocatalytic reactions were performed by dispersing 20 mg of catalysts in a 100 mL 10% aqueous solution of lactic acid (10 mL) and water (90 mL). The solution was bubbled with 5% CH_4/Ar to remove the dissolved oxygen prior to irradiation under a 500 W UV-vis lamp. Throughout the irradiation process, agitation of the solution ensured uniform irradiation of the samples. A 30 mL sample of the generated gas was collected and analysed by gas chromatograph.

The composition of gas produced from all samples was tested using a Gas Chromatograph (GC) fitted with both a Thermal Conductivity Detector (TCD) and a Flame Ionisation Detector (FID). This allowed for accurate detection of H_2, Ar, CH_4 and identification of other species that may have been present (N_2, CO_2 and O_2).

Static PL and TRPL measurements: Instrumental setups for femtosecond time-resolved and nanosecond time-resolved photoluminescence (denoted as fs-TRPL and ns-TRPL, respectively) have been described previously.[6,7] Briefly, these measurements were performed based on a commercial Ti:Sapphire regenerative amplifier laser system. The 350 nm pump pulse (~100 fs) was produced by an optical parametric amplifier (OPA) pumped by the 800 nm fundamental (40fs, 1kHz) generated by the Ti:Sapphire laser system. The fs-TRPL were achieved by employing a gated method called the Kerr-gate technique.[6] A Kerr device comprising a 1 mm thick Kerr medium (quartz) equipped within a crossed polarizer pair was driven by an 800 nm laser pulse (named the probe pulse) to function as an ultrafast optical shutter to sample transient PL spectra at various selected pump/probe delays. Temporal delay of the probe to pump pulse was controlled by a computer controlled optical delay line. The fs-TRPL signals were collected by a spectrograph and detected with a liquid nitrogen cooled CCD detector. For the ns-TRPL measurement, an intensified CCD (ICCD) detector, which was synchronized to the fs laser system, was used to detect transient PL spectra at designated time intervals after the photo-excitation. The instrument response function (IRF) was ~150 fs for the fs-TRPL and ~2 ns for ns-TRPL. The static PL spectra were acquired by a Jobin Yvon FluoroMax-4 spectrofluorometer with a home-built powder sample holder for quantitative measurement of PL spectra and intensity. All the measurements were performed at room temperature and atmospheric pressure with a solid state sample.

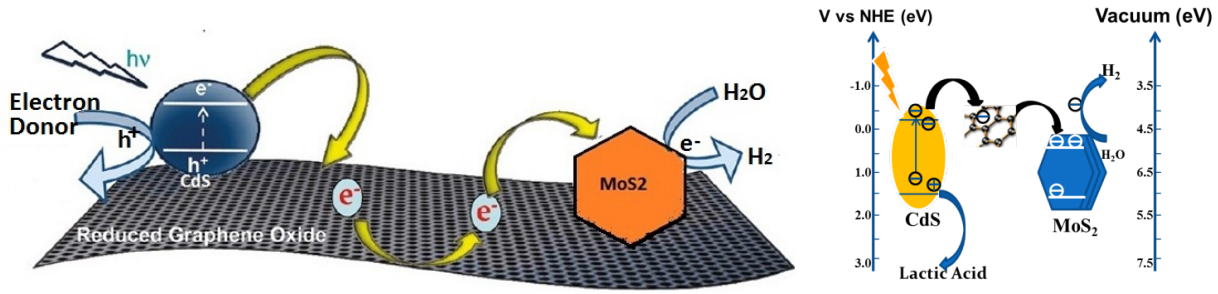

Scheme 1. Graphene supported CdS and MoS_2 for photocatalytic hydrogen evolution.

3. Figures

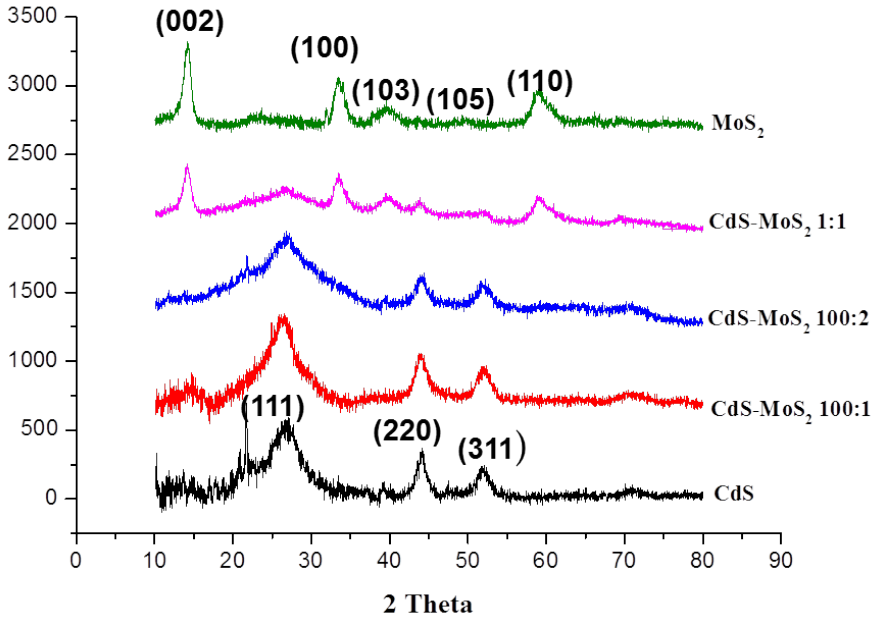

Figure S1. X-Ray Diffraction of MoS_2, CdS and CdS-MoS_2

Figure S1 shows the XRD patterns of CdS nanoparticles, MoS_2 and CdS-MoS_2 (mass ratio of 100:1, 100:2 and 1:1). The peaks at 26.6°, 44.0°, and 52.3° correspond to the diffractions of the (111), (220), and (311) planes of cubic CdS, respectively.[8] All the diffraction peaks of MoS_2 are well indexed according to the hexagonal MoS_2 phase.[9] For 100:1 and 100:2 CdS-MoS_2, no characteristic diffraction peaks for MoS_2 are observed because of the low amount and relatively low diffraction intensity of MoS_2. However we can see all the characteristic peaks of CdS and MoS_2 without new peaks in the 1:1 CdS-MoS_2 hybrid, indicating there is no new phase produced in the preparative procedure.

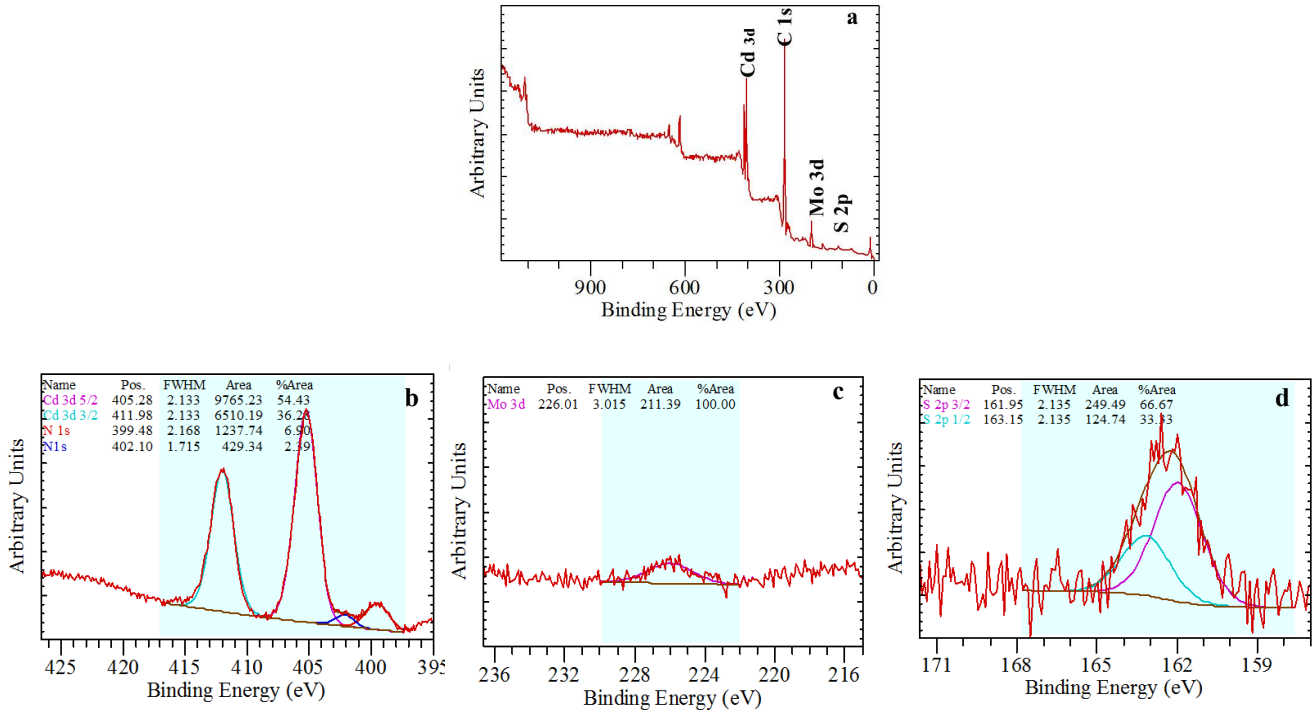

Figure S2. XPS spectra for (a) a survey scan of CdS-graphene-MoS_2 composite (100:0.4:2), and high resolution XPS of the (b) Cd 3d region (c) Mo 3d region and (d) S 2p region.

All XPS peaks are referenced to the C 1s of adventitious carbon from the XPS instrument. A typical high resolution XPS spectrum of Cd 3d is shown in Figure S2 (b). Two peaks at 405.3 and 412.0 eV are assigned to Cd 3 $d_{5/2}$ and 3 $d_{3/2}$, which are characteristic peaks of Cd^{2+} in CdS. As for the high resolution spectrum of Mo 3d (c), the small peak at 226.0 eV is attributed to Mo 3d. This peak is not obvious because of the low amount of MoS_2 (about 2%) in the composites. Figure S2 (d) shows the XPS spectrum of the S 2p region, which can be fitted into two peaks: S $2p_{3/2}$ and S $2p_{1/2}$, which appear at 162.0 and 163.2 eV, respectively. The XPS results further confirm the coexistence of MoS_2 and CdS in the composites, which is consistent with the XRD results.

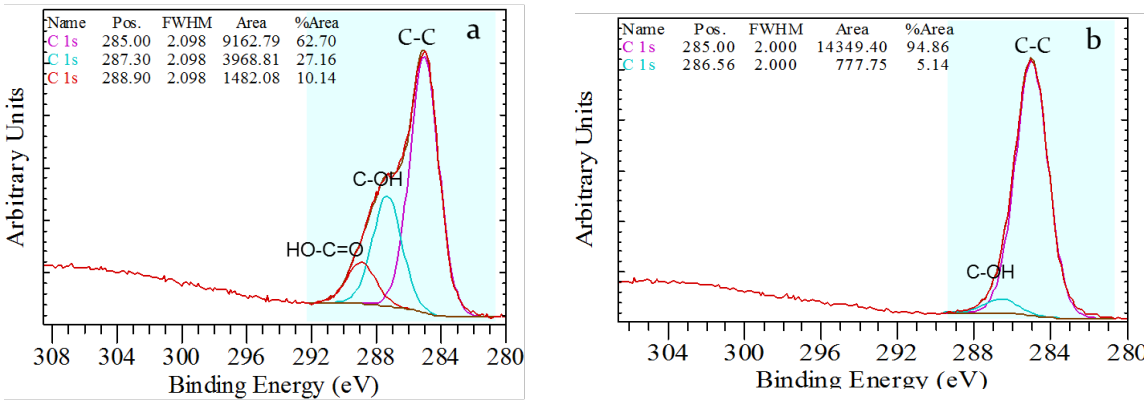

Figure S3. High-resolution XPS spectra of C 1s region from synthesised graphene oxide (a) and CdS-graphene-MoS_2 (100:0.4:2) (b)

The XPS analysis above can be used to determine surface elemental composition of complex mixtures. Table S1 shows the atomic percentages for each elements on a typical CdS-graphene-MoS_2 composite using calibrated signals of C 1s, O 1s, Cd 3d, S 2p and Mo 3d. The analysis presented in Fig. S2 indeed suggests that CdS and MoS_2 are successfully deposited on graphene sheets. Notice from Table S1 that the O/C atomic ratio is about 0.37 for pure graphene oxide. However, the CdS-graphene-MoS_2 contains almost no oxygen, which suggests that there was an extensive reduction of graphene oxide during the preparation. The apparent decrease in oxygen content was also detected by comparing the change in high-resolution XPS of C 1s of graphene oxide with the composite product. As shown in Fig. S3,

the oxygen containing functional groups, hydroxyl (C-OH) and carboxyl (O=C-OH) have been attenuated substantially, indicating the reduction of graphene oxide by ethanol during the preparation.

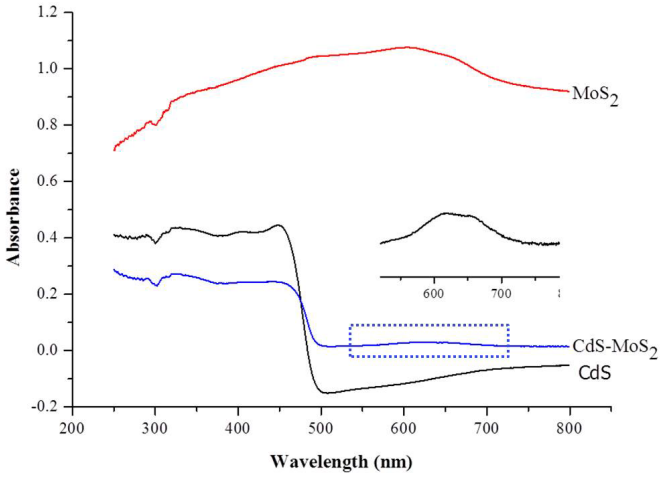

Figure S4. UV-vis absorption spectra of CdS, MoS_2 and CdS-MoS_2 (100:2) samples

Figure S4 shows UV-vis absorption spectra of CdS, MoS_2 and CdS-MoS_2 (100:2) samples. CdS can absorb visible light with wavelengths shorter than 480 nm and displays a steep absorption, indicating the narrow size distribution of CdS nanoparticles.[9] The CdS-MoS_2 hybrid is characterised with some broad absorption from 550-700 nm (see insert) due to the narrower indirect bandgap of MoS_2.[10]

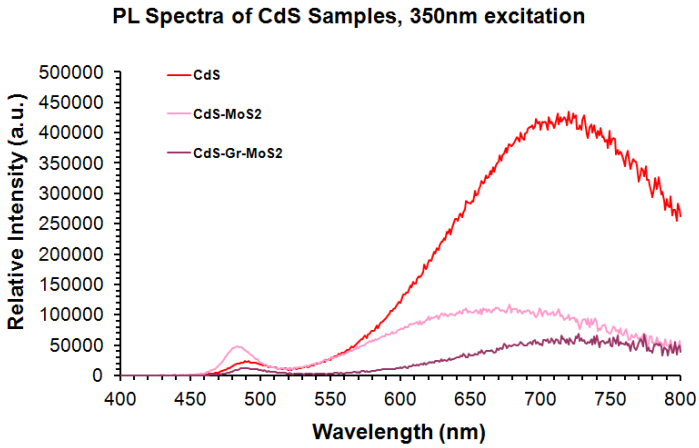

Figure S5. Static PL spectra of CdS, CdS-MoS_2 (100:1) and CdS-graphene-MoS_2 (100:0.2:1) samples

Figure S5 shows the static PL spectra of CdS, CdS-MoS_2 (100:1) and CdS-graphene-MoS_2 (100:0.2:1) samples. The significant quenching of intense emissions from CdS, in particular in the 550-800 nm region (recombination over trap sites) by MoS_2 and graphene, is noted.

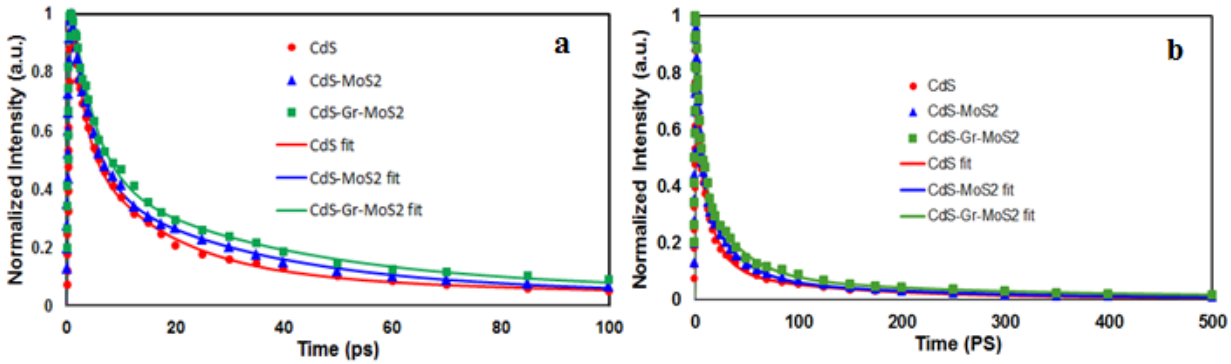

Figure S6. fs-TRPL decay curves at ~490 nm in (a) 0-100 ps and (b) 0-500 ps for CdS, CdS-MoS_2 (100:1) and CdS-graphene-MoS_2 samples (100:0.4:1).

Figure S6 shows the experimental (Δ, ○, □) and fitted (solid lines) fs-TRPL decay curves at ~490 nm in (a) 0-100 ps and (b) 0-500 ps for CdS, CdS-MoS_2 (100:1) and CdS-graphene-MoS_2 samples (100:0.4:1). The fitting parameters for the decay curves are shown in Table S2 (fs-TRPL) and Table S3 (ns-TRPL).

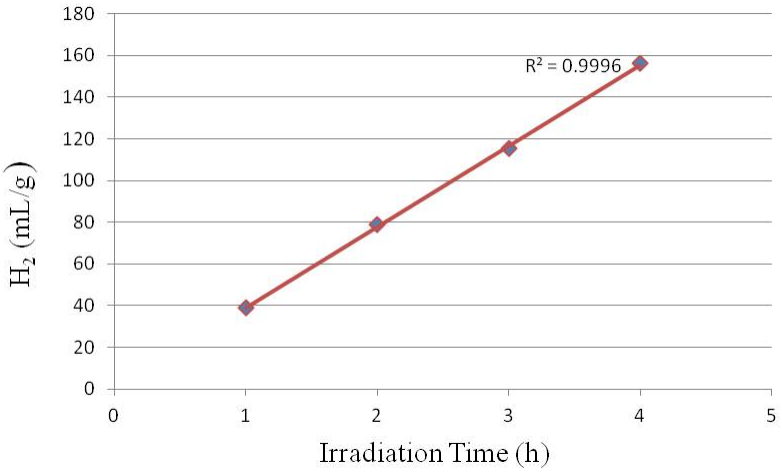

Figure S7. Linear correlation between hydrogen production and reaction time for CdS-Graphene-MoS_2

Figure S7 shows the linear correlation between total hydrogen production and reaction time for CdS-Graphene-MoS_2 (100:0.4:1).The amount of H_2 evolved increases linearly with the reaction time during the first 4 hours of testing.

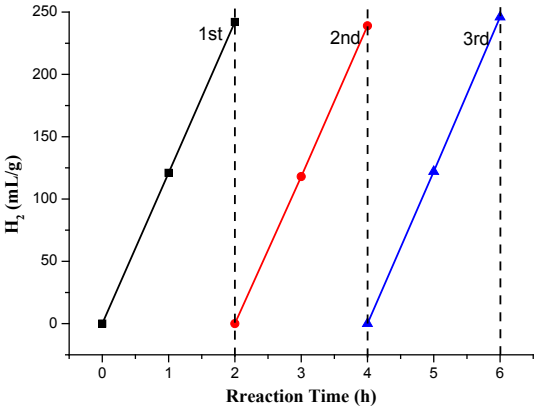

Figure S8. Stability measurements of CdS-graphene-MoS_2

Figure S8 shows three identical H_2 evolution rates measured over three 2 h repeated irradiation cycles, indicating the stability of CdS-graphene-MoS_2 (100:0.4:2) Although a longer period of testing is more desirable to demonstrate its durability, the instability in our lamp intensity and excessive heat generated would preclude it for unattended operation.

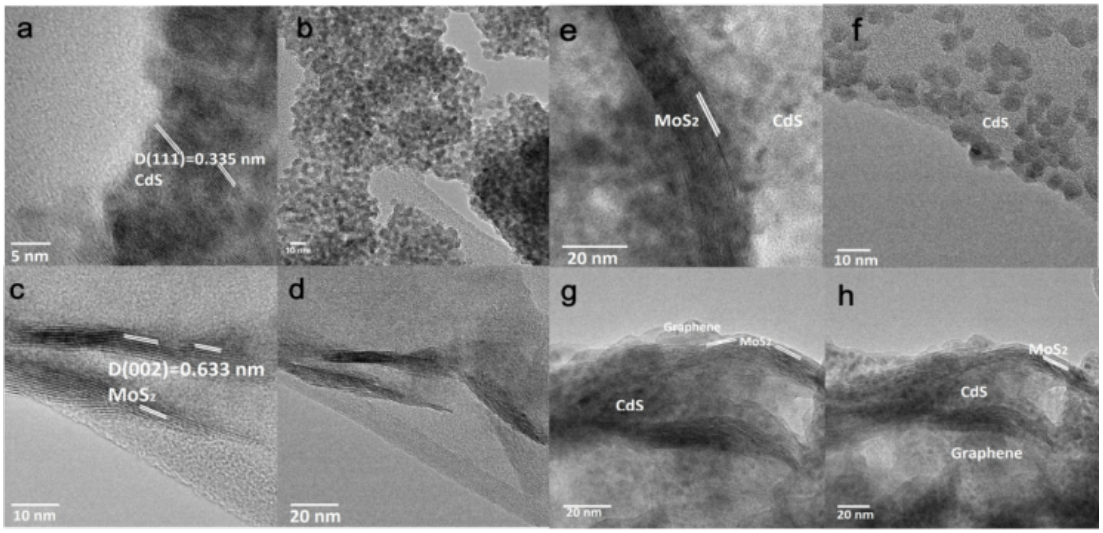

Figure S9 TEM and HRTEM images for (a,b) CdS; (c,d) MoS_2; (e,f) CdS-MoS_2 (100:2); (g,h) CdS-graphene-MoS_2 (100:0.4:2).

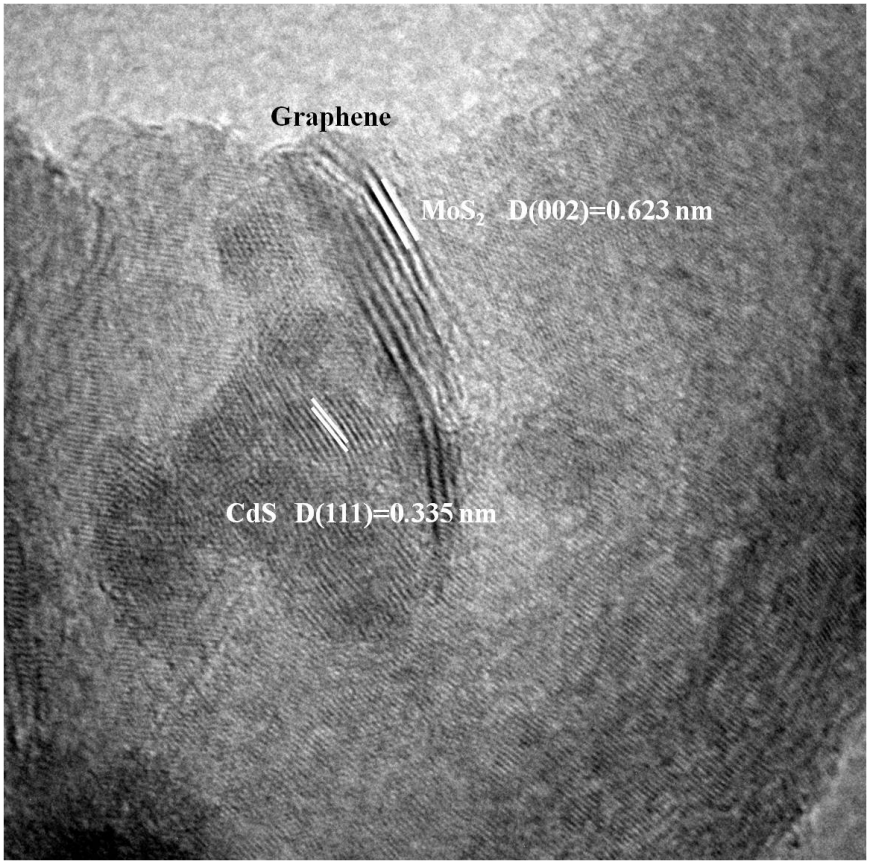

Figure S10 HRTEM image of CdS-graphene-MoS_2 where CdS and MoS_2 on graphene with fringes corresponding to (111) CdS and (002) MoS_2 are clearly visible.

Figures S9-10 show the high resolution images of CdS-graphene-MoS_2 where lattice fringe distances of CdS and MoS_2 on graphene correspond to those of XRD data are evident.

4. Tables

Table S1. The elemental composition of prepared samples

Element	Graphene Oxide (%)	CdS (%)	MoS_2 (%)	CdS-MoS_2 (weight %) (100:2)	CdS-Gr-MoS_2 (weight %) (100:0.4:2)
O	27.0	0	13.5	0	0
C	73.0	0	0	0	93.6
Cd	0	45.5	0	57.1	4.9
Mo	0	0	32.4	4.8	0.1
S	0	54.5	54.1	38.1	1.3

Table S2. The fitting parameters for the decay curves (fs-TRPL)

	CdS		CdS-MoS_2		CdS-Gr-MoS_2	
τ_1, ps (a_1)	2.0	(0.56)	3.6	(0.63)	4.3	(0.61)
τ_2, ps (a_2)	15.3	(0.36)	28.5	(0.31)	33.7	(0.32)
τ_3, ps (a_3)	123	(0.08)	191	(0.06)	225	(0.07)
τ_{av}, ps	16.5		23.2		28.8	

Table S3. The fitting parameters for the decay curves (ns-TRPL)

	CdS		$CdS-MoS_2$		$CdS-Gr-MoS_2$	
τ_1, ns (a_1)	0.9	(0.24)	1.6	(0.44)	1.3	(0.36)
τ_2, ns (a_2)	6.2	(0.18)	9.8	(0.22)	6.6	(0.35)
τ_3, ns (a_3)	51.5	(0.25)	45.8	(0.16)	46.3	(0.18)
τ_4, ns (a_4)	398	(0.22)	206	(0.11)	218	(0.08)
τ_5, ns (a_5)	942	(0.08)	755	(0.06)	773	(0.03)
τ_6, ns (a_6)	2404	(0.02)	2480	(0.01)	3023	(0.01)
τ_7, ns (a_7)	8933	(0.002)	9352	(0.001)	12141	(0.001)
τ_{av}, ns	239		116		86	

We analyzed the fs-TRPL decay data (decay profiles at time intervals from 0 to 6000 ps). The experimental and fitted decay profiles for samples CdS, CdS-MoS_2 (100:1) and CdS-graphene-MoS_2 samples (100:0.4: 1) at varied timescales are shown in Fig S6(a) (0 to 100 ps) and (b) (0 to 500 ps), the time constants (τ_i) and associated amplitudes (a_i) derived from the fittings are listed in Table S2. The decay profiles of 490 nm fs-TRPL (due to the band edge emission) can be well fitted with multi-exponential functions (after convoluted with the IRF) for CdS and the two other samples. In all three samples, the three decay times (fraction contribution), e.g., τ_1~2.0-4.3 ps (~56-63%), τ_2~15.3-33.7 ps (~31-36%), and τ_3~123-225 ps (~6-8%) are generally observed with an increasing average decay time ($\tau_a=\sum\tau_i \cdot a_i$) from 16.5 ps, 23.2 ps and 28.8 ps for CdS, CdS-MoS_2 and CdS-graphene-MoS_2 samples, respectively (Table S2). Clearly, the decay is mostly due to the fast components τ_1 and τ_2. The progressive longer lifetimes (τ_1 and τ_2) in the presence of MoS_2 and MoS_2-graphene are assigned to the interaction of the excited electrons from irradiated CdS with these materials (attenuating the non-radiative recombination processes such as Auger relaxation at this time-scale).[11] The effect of electron transfer from excited CdS to MoS_2-graphene is more pronounced in the ns-TRPL spectroscopy as well as the quenching of static PL in the presence of MoS_2 and MoS_2-graphene (Table S3).

References

(1) Joo, J.; Na, H. B.; Yu, T.; Yu, J. H.; Kim, Y. W.; Wu, F.; Zhang, J. Z.; Hyeon, T. *J. Am. Chem. Soc.* **2003**, 125, 11100.

(2) Xiang, Q.; Yu, J.; Jaroniec, M. *J. Am. Chem. Soc.* **2012**, 134, 6575.

(3) Marcano, D. C.; Kosynkin, D. V.; Berlin, J. M.; Sinitskii, A.; Sun, Z.; Slesarev, A.; Alemany, L. B.; Lu, W.; Tour, J. M. *Acs Nano* **2010**, 4, 4806.

(4) Hummers, W. S.; Offema, R. E. *J. Am. Chem. Soc,* **1958**, 80, 1339.

(5) Coleman, J. N. et al. Science, **2011**, 331, 568.

(6) C. Ma, C. T. L. Chan, W. M. Kwok, C. M. Che, Chem. Sci., 2012, 3, 1883.

(7) T. Zhang, X. Zhu, C. C. W. Cheng, W. M. Kwok, H. L. Tam, J. Hao, D. W. J. Kwong, W. K. Wong, K. L. Wong, J. Am. Chem. Soc., **2011**, 133, 20120.

(8) Q. Li, B. Guo, J. Yu, J. Ran, B. Zhang, H. Yan, J. Gong, J. Am. Chem. Soc., **2011**, 133, 10878.

(9) Y. Li, H. Wang, L. Xie, Y. Liang, G. Hong, H. Dai, J. Am. Chem. Soc. **2011**, 133, 7296.

(10) F. A. Frame, F. E. Osterloh. J. Phys. Chem. C **2010**, 114, 10628.

(11) Marco Marceddu et al., Nanotechnology **2012**, 23, 015201.